LA-UR-81-3144

MASTER

TITLE: ELMO BUMPY TORUS FUSION-REACTOR DESIGN STUDY

AUTHOR(S): Robert A. Krakowski and Dale DeFreece

SUBMITTED TO: 9th Symposium on Engineering Problems of Fusion Research
(October 26-29, 1981) Chicago, Illinois

University of California

LOS ALAMOS SCIENTIFIC LABORATORY
Post Office Box 1663 Los Alamos, New Mexico 87545
An Affirmative Action/Equal Opportunity Employer

Form No. 836 R3
St. No. 2629
12/78

UNITED STATES
DEPARTMENT OF ENERGY
CONTRACT W-7405-ENG. 36

ELMO BUMPY TORUS FUSION-REACTOR DESIGN STUDY*

Robert A. Krakowski and Dale DeFreece**
Los Alamos National Laboratory
Los Alamos, NM 87545

Summary

A complete power plant design of a 1200-MWe ELMO Bumpy Torus Reactor (EBTR) is described. Those features that are unique to the EBT confinement concept are emphasized, with subsystems and balance-of-plant items that are generic to magnetic fusion being adopted from past, more extensive tokamak reactor designs. This overview paper stresses the design philosophy and assumptions that led to an economic, 35-m major-radius design that at 1.4 MW/m^2 wall loading generates 4000 MWt with a 15% recirculating power fraction.

Introduction and Background

The ELMO Bumpy Torus (EBT) concept[1] is a toroidal array of simple magnetic mirrors. An rf-generated, low-density, energetic electron ring at each position between mirror coils (i.e., midplane location) stabilizes the bulk, toroidal plasma against well-known instabilities associated with simple mirror confinement. The EBT reactor was first examined over four years ago.[2] Revisions of this first design have been made during the intervening years.[3-6] The utilization of advanced fusion fuels in a bumpy-torus reactor has also been considered.[7] Interim results from the study reported here have been reported elsewhere,[8] and the detailed account of this study is given in Ref. 9.

The presence of a high-beta electron ring at each midplane position is crucial to the MHD stability of the bumpy torus. A local region of minimum average field is created by the rings, giving an MHD-favorable decrease in the quantity $\oint dl/B$ with increasing radius. Although this region of minimum-average field does not extend to the centerline of the toroidal plasma, it can be argued that a region of stable bulk plasma extends to the magnetic axis.[4,10,11] The stability of the high-beta toroidal plasma has been inferred[10] to be limited by a value of the bulk-plasma beta that approximately equals the electron-ring beta. Although these stability-related beta limits are based upon the assumption of rigid rings and are sensitive to the assumed pressure profiles, these results serve as the primary stability constraint applied to this EBTR study. A more recent computation[12] however, has raised some questions with respect to this simple stability criterion, although the quantitative implications of this recent theory on the reactor performance could not be made within the time schedule of the present study.

The diffusive loss of particles and energy from the nonaxisymmetric bumpy-torus configuration is determined by neoclassical processes in which the fundamental diffusive step size is influenced significantly by the magnitude and direction of guiding-center particle orbits in a toroidal geometry in the presence of both local magnetic field gradients and radial (ambipolar) electric fields. The neoclassical expression for the confinement time reflects a favorable scaling for the Lawson parameter, $n\tau_p$, that increases with temperature, T, to the 3/2 power and with the square of the magnetic aspect ratio, R_T/R_c. The neoclassical transport scaling is examined in more detail in Ref. 9,13-18, and lies at the heart of this EBTR study.

As for all conceptual fusion reactor designs, the determination of an operating point requires the unique combination of applied plasma physics (particle/energy transport, stability, equilibrium) and plasma engineering (burn simulation and control, fusion yield and first-wall energy fluxes, fueling, impurity control). In order to meet these requirements simultaneously, the determination of an EBTR design point has coupled burn, transport, magnetics, electron-ring, and blanket/shield models that represent a simplification of a non-axisymmetric three-dimensional geometry. The iteration and optimization between physics and engineering occurred with the concurrent numerical evaluation of models describing the mechanical/stress response of the magnets, the performance of the impurity control scheme, and the thermal-mechanical response of the blanket. Simultaneously, key physics and engineering constraints were monitored in conjuction with those aspects of plant layout that might interfere with the goals of system access and maintainability. Lastly, a fully parametric systems code was developed and used in parallel to this iterative scheme in order to estimate and optimize total system cost and cost-of-electricity (COE). This process continued until a relatively self-consistent design point emerged, with major uncertainties being quantified and documented wherever possible.[9] The major physics assumptions adopted by this study are summarized below.

- Neoclassical transport modeled in zero-dimensions (Kovrizhnykh electrons, plateau ions, and assumed density and temperature gradient scale lengths).
- Vacuum magnetic field model in toroidal geometry to describe the toroidal field and ARE coils; averaging used to reduce to zero-dimensional transport parameters.
- Classical theory describes relativistic electron-ring losses.
- First-harmonic electron-ring heating.
- Stability limit given by average plasma beta of ≤ 0.20 (midplane beta ≤ 0.45), as predicted by stability theories based on non-deformable rings.
- Steady-state plasma operation (alpha particles are thermalized classically and transported neoclassically) after a simulation of plasma startup.
- Use of circular and off-set ARE-coil configurations.

The following engineering-design ground rules were adopted.

- 10th commercial plant, 1200 MWe.
- Steady-state operation (77% plant factor).
- Pressurized-water-cooled, solid-breeder blanket.
- Pumped limiter for impurity control.
- Life-of-plant superconducting coils.
- ARE coils used to minimize physical size of power plant.
- RF bulk heating for startup and electron rings.
- Fully remote maintenance.

*Work performed under auspices of the U.S. Department of Energy.

**McDonnell Douglas Astronautics Company, St. Louis, MO.

Reactor Design

The recent completion of a similar but more extensive conceptual design of a commercial tokamak power plant[20] by a majority of the EBTR design participants was of great benefit to this study. This overlap allowed the utilization of applicable experience and analysis for similar systems while maximizing the design effort on systems that are unique to EBTR. This combination of design resources also allowed quantitatively meaningful comparisons to be made between the EBTR design and the more extensive STARFIRE design.[20] Most of the buildings envisaged for both concepts are identical in function and form, except for the reactor and electrical equipment buildings. The site requirements and boundaries for all commercial magnetic fusion power applications are considered to be identical. The turbine plant, electrical plant, and miscellaneous plant equipment for EBTR are identical to that selected for the STARFIRE fusion power plant. The tritium fuel handling and storage system developed for the STARFIRE design is also applied to the EBTR concept.

Design Overview

One of the major advantages of the EBT reactor is the high aspect ratio, which allows easier reactor maintenance schemes. The effective utilization of the access area around the torus is a major design goal. The torus elements are wedge-shaped, requiring the blanket and/or shield to be removed radially outward. In order to provide outboard accessibility for maintenance and assembly, the structure needed to restrain induced magnetic loads is incorporated largely on the inboard side of the reactor.

Another key design premise is the minimization of the vacuum volume. A realistic design that allows a vacuum boundary at the first wall could not be identified, because of radiation damage to a welded joint or vacuum seal located at or near the first wall and the inaccessibility of the vacuum seal for maintenance. The use of the reactor containment room as a vacuum vessel has the disadvantage of large vacuum environment and pumping requirements, extensive surface areas for tritium entrapment, and the difficulties of operating support equipment under vacuum conditions. Elimination of these options places the vacuum boundary within the blanket and shield region.

To maximize the system credibility and to utilize effectively the relatively small design effort allocated to this study, a conventional PWR heat transfer and transport system is utilized. Specific design details were modified relative to the similar STARFIRE tokamak design[20] in order to accommodate the unique aspects of the EBTR approach (e.g., incorporation of the pumped-limiter/feed-water heating scheme).

Reactor Design Point

The models and physics/technology constraints developed in the course of this study,[9] were used to examine a range of reactor operating points that promise economic power near 1200 MWe (net). Table I summarizes the specific design that has emerged from this study. A cost comparison with the STARFIRE design[20] is given in Ref. 9. Although considerably more effort was devoted to the latter study, the fact that the costing data base and costing/design procedures are similar makes such a comparison meaningful. Although this EBTR design operates with lower plasma, first-wall, and blanket power densities than STARFIRE (4.13 MWt/m^3, 1.4 MWt/m^2, and 3.33 MWt/m^3, respectively for EBTR versus 4.50 MWt/m^3, 3.6 MWt/m^2, and 6.46 MWt/m^3 for STARFIRE), the system power densities are comparable (0.50/0.24 MWt/m^3 without/with ARE-coil volume for EBTR versus 0.30 MWt/m^3 for STARFIRE), because the total thermal power and the volume enclosed by the coils are comparable for EBTR and STARFIRE (4028 MWt and 7978/16441 m^3 without/with ARE coils for EBTR and 4033 MWt and 13443 m^3 for STARFIRE, respectively). Consequently, the total direct costs, the unit capital costs, and the cost-of-electricity are similar (2108 M$, 2366 $/kWe, and 38.9 mills/kWeh for EBTR versus 1726 M$, 2000 $/kWeh and 35.1 mills/kWeh for STARFIRE, respectively).

Reactor and Balance-of-Plant Layout

The EBTR power plant contains all the necessary elements of a central generating facility: reactor, turbine plant, electric plant, control and administration areas, maintenance services, heat-rejection systems, and supporting utilities. A nominal 1000-acre tract was selected for the plant that provides adequate space for additional generating units. The Reactor Building is centrally located within the plant site. The turbine, Hot Cell, cryogenics, and fuel handling equipment are located close to the Reactor Building in order to minimize piping lengths. Wet, natural-draft cooling towers are used. The site is located near a river to provide both adequate makeup water and the means to ship the large, heavy components to the site during construction.

Early EBTR concepts[2] were considered to be large-aspect-ratio devices, with a major radius of 60 m or more. For a device of that radius, the Reactor Building dominates the site plan and the plant economics. In this study, a concerted effort is made to reduce the size of the reactor in order to enhance the economics while preserving the attractive maintenance features of a high-aspect-ratio machine. This design explicitly incorporates ARE coils to reduce the major radius by a factor of ~ 2 while maintaining the same magnetic aspect ratio and acceptable plasma transport.

Each of 36 reactor sectors is comprised of two different modules: a midplane blanket/shield module, located between the toroidal-field (TF) coils, and a coil-plane blanket/shield module. All 72 modules are physically and thermohydraulically isolated from each other except for a welded, intersector vacuum seal located outside the shield. By disconnecting coolant lines, vacuum lines, and rf-heating waveguides, the midplane module can be withdrawn radially outward. After the midplane module is removed, the coil-plane module can be withdrawn toroidally from the TF/ARE-coil assembly followed by a radial translation outward. This design approach allows each 726-tonne TF/ARE-coil assembly, which requires precise alignment, to remain fixed while blanket/shield replacement is accomplished.

A factor of two aspect-ratio enhancement dictates a high ARE-coil current and, hence, large coil cross section and stored energy (131 GJ). To minimize the support structure connecting the ARE and TF coils and to eliminate the transition between cold and warm structure, the set of one TF and two ARE coils is enclosed in a single cryogenic vessel with interconnecting cryogenic support structure. Although this approach creates a large and heavy coil set, it reduces the interconnecting and mounting structure, alignment and installation problems, cryogenic requirements, and manufacturing and quality-control needs. The coil casing also supports and aligns the coil-plane blanket/shield module. The two ARE and one

TABLE I
EBTR MAJOR DESIGN PARAMETERS

Net electrical power (MW)	1214
Gross electrical power (MW)	1430
Total thermal power (MW)	4028
Gross power-conversion efficiency (%)	35.5
Overall plant availability (%)	[illegible]
Major radius (m)	3[illegible]
Plasma radius (average) (m)	[illegible]
Plasma volume (m^3)	[illegible]
Number of sectors	[illegible]
Maximum field at magnet (T)	9.7
Field on axis (coil-plane/midplane, T)	5.03/2.25
Average toroidal beta	0.17
Midplane beta	0.46
Mirror ratio	2.24
Average DT ion density ($10^{20}/m^3$)	0.95
Average DT ion temperature (keV)	27.9
Plasma burn mode	Continuous/ignited
Plasma heating method (startup)	Lower hybrid (rf, 0.5-1.4 GHz)
Ring heating method	ECRH, (rf, 50 GHz)
Ring heating power absorbed (MW)	42
Plasma impurity control method	Vacuum-pumped limiter
First-wall/blanket structural materials	Advanced austenitic stainless steel
Neutron wall loading (MW/m^2)	1.4
Tritium breeding medium	natural α-$LiAlO_2$
Primary coolant	Pressurized water
Thermal conversion method	Steam

TF coils within each coil set are connected electrically in series to reduce the out-of-plane loads that would occur if one of the coils should fail.

The blanket/shield design approach results from constraints imposed by maintainability as well as those imposed by physics constraints. In order to achieve acceptable transport in a relatively small torus with ARE-coil currents that are not excessive relative to the TF-coil current (i.e., $|I_{ARE}/I_{TF}| \leq 0.25$), it is desirable to locate the TF coils as close to the plasma as is possible. Hence, the thinner inboard coil-plane blanket/shield design emphasizes the shielding function, with that portion of the blanket having a tritium breeding ratio below unity. A net tritium-breeding ratio greater than unity (i.e., TBR $\geq$ 1.06) is achieved by enhancing tritium production in the outboard coil-plane and midplane blanket/shield regions. This results in a blanket/shield design that consists of offset cylinders and wedge-shaped sections in the coil plane and concentric cylinders in the midplane.

A pumped-limiter impurity-control system instead of a magnetic divertor was selected to avoid possibly detrimental perturbations of the magnetic topology. Several configurations and locations of pumped limiters were assessed. The selected configuration utilizes two poloidal limiters for each sector in conjunction with vacuum slots located at the junction between the coil-plane and midplane modules. Impurities and neutralized DT atoms are pumped through these poloidal limiter slots into an annular plenum formed between the blanket and shield assemblies. The vacuum cryopumps are attached directly to the shield, thereby providing an acceptable pumping path with high vacuum conductance.

The first-wall/blanket configuration and material choices are based on a PWR coolant and heat-transport system. The structural material is Primary Candidate Alloy Stainless Steel (PCASS). The neutron-multiplier is metallic beryllium, and the solid breeder is natural $LiAlO_2$. On the basis of these configurational and material choices, the blanket has a theoretical breeding ratio of 1.06 and an energy multiplication of 1.5. The shielding configuration under the TF coils in the inboard region is most critical because of the need to minimize transport losses by locating the coils as close as possible to the plasma surface; a compact but effective shield is used in this region. This design goal is accomplished by using a small amount of tungsten/lead mixture as a local shielding material in the inboard coil region. The shield elsewhere is stainless steel, TiH_2, TiB_2, and water. Local shielding regions are provided to assure minimal neutron penetration through joints and ducts.

The EBTR plasma is proposed to be driven to ignition by lower-hybrid heating (LHH) with a variable (tunable) frequency of 0.55-1.40 GHz; the LHH is applied symmetrically in four sectors around the torus. After ignition the plasma is assumed not to require bulk heating. The electron rings require continuous energy input sustenance against radiation and collisional-drag losses. This power is supplied by ECRH at a frequency of 50 GHz (first harmonic) in each of the 36 sectors. Gyrotrons and crossed-field amplifiers are located directly inboard of the reactor to assure minimal power losses in the respective waveguides.

A three-dimensional cutaway drawing of the reactor building and the key reactor and support subsystems is shown in Fig. 1. Sections of the reactor are shown both during construction and in a completed state. This cutaway view illustrates the close fitting of the reactor to the reactor building inner wall in order to reduce building costs and reactor structural supports. The reactor support structure, including the pedestal that supports the midplane module, coil support arms, and coil gimbal supports, are shown both prior to and following installation of the coil sets and modules. The more massive arms support the coil sets, while tension struts support the midplane modules. One coil set and coil-plane blanket/shield module are shown in section in order to illustrate the blanket/shield closely surrounded by the TF coil. The cryogenic intercoil structure consists of I-beams and trusses and can be seen in the sectioned view of the coil set,

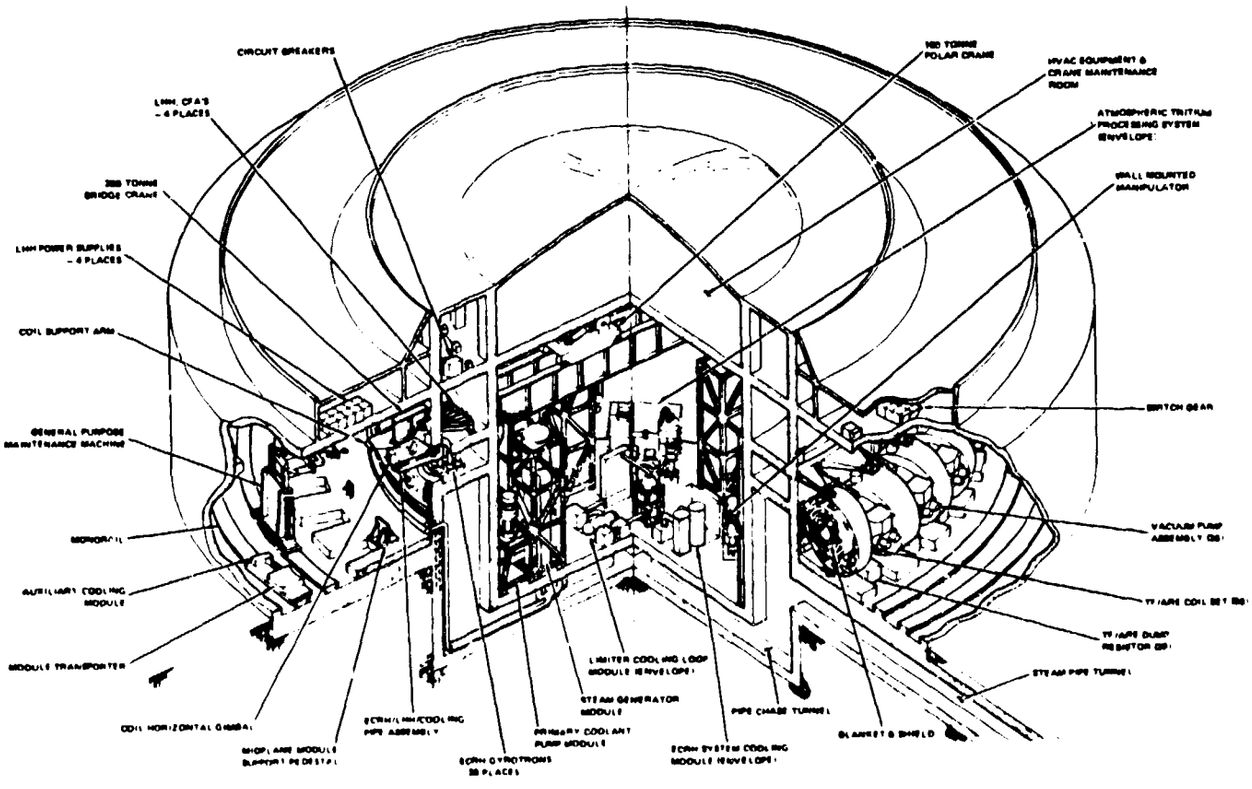

Fig. 1. EBT Reactor Building showing the interrelation of key reactor components.

although the ARE coil is largely hidden from view. Positioned between the elevated (1.?-m) concrete support bases for the coil sets are the TF/ARE-coil dump resistors. Ample maintenance access is provided outboard of the reactor for maintenance machines and module transporters that are mounted on monorails. Overhead in the reactor hall are two bridge cranes (a portion of one is shown); these cranes assist in construction and maintenance of the reactor. The illustrated arrangement of the reactor and associated systems is designed to provide a synergistic and cost-effective utilization of space within the reactor hall as well as within the control room of the reactor building.

Conclusions

The composite result of this study forms the base for an attractive fusion power system. Further conceptual design and systems efforts should prove fruitful in improving the prospects of EBT as a power system. A synopsis of the study conclusions is presented below.

- The economic evaluation indicates that the capital cost and COE for an EBT commercial power plant are comparable to the better developed and understood tokamak concept.[20] Additionally, the COE is considered to be competitive with energy produced by new fission or fossil power plants. As future refinements are incorporated, the competitive position for EBT is expected to be further enhanced.
- The high-aspect-ratio feature of the EBT assures a highly accessible and maintainable reactor with totally remote maintenance operations, while promising a plant availability equal to or greater than present fission plants.
- A compact, integrated reactor building was developed based upon the unique reactor features of the EBT concept. The use of conventional power-conversion and balance-of-plant systems is possible, illustrating a compatibility with conventional power systems.
- Blanket material selection and configurational tailoring accomplished adequate tritium breeding, while maintaining a magnetics geometry needed to obtain the required plasma confinement. This blanket shield configuration was achieved using a natural $LiAlO_2$ solid breeder because of cost and safety considerations.
- An integrated TF/ARE-coil design is proposed that meets all major magnetics/transport requirements. This TF/ARE-coil set adequately reacts the induced magnetic-force loading and retains a fully remote maintenance capability, although the coils are designed to function as life-of-plant components.
- Magnetic aspect ratios, R_T/R_c, of 15 to 20, required for adequate plasma confinement, can be achieved for a reactor with a 35-m major radius, while meeting necessary engineering constraints. This configuration is accomplished using a significant amount of ARE current ($I_{ARE}/I_{TF} \sim -0.22$) for the design point. Alternatively, this configuration may be achieved by designing for larger mirror ratios. An important physics/engineering/cost tradeoff exists, which requires further study.
- The pumped limiter appears to be an attractive impurity-control concept for EBTs. Although many of the coupled plasma/scrape-off/limiter/plot processes remain to be demonstrated experimentally, the results of the phenomenological description provide promising indications of feasibility.

- Trends derived from the systems code analysis are evident that promise an improved competitiveness of future designs. These trends include the following:
  - Cost optimizes on the maximum average beta, β, consistent with the mirror ratios used (i.e., maximum allowed midplane beta, $\beta = 4\beta_{MP}/(1 + M)^2$).
  - A strong dependence of cost on the maximum allowable mirror ratio is indicated.
  - Cost-optimized designs for constant beta are found when the number of sectors and ARE-coil current are reduced and simultaneously, the toroidal magnetic field and plasma radius are increased.
  - EBT exhibits a stronger economy of scale than a tokamak at the 1200-MWe(net) design point.
  - The optimum value for ARE-coil current appears to be in the range $|I_{ARE}/I_{TF}| = 0.08 - 0.16$, where a broad minimum occurs. Lower values tend to increase cost because of increased torus radius and higher values tend to increase cost because of higher magnet costs.
- Several physics issues/questions/uncertainties can significantly affect the EBT reactor viability: magnetics/transport in high-beta plasma, alpha-particle dynamics, electron-ring energy losses and general stability, profile effects, edge-plasma physics, plasma heating/fueling during startup and approach to ignition, and steady-state plasma burn control. The coupling between core-plasma beta at the ring location, ring volume (thickness), average core beta and radial profiles remains a particularly crucial physics issue for EBT.

References

1. R. A. Dandl, J. L. Eason, H. O. Eason, P. H. Edmonds, A. C. England, W. J. Herman, and N. H. Lazar, "Electric Cyclotron Heated "Target" Plasma Experiments," Proc. 3rd Intern. Conf. on Plasma Physics and Controlled Nuclear Fusion Research, II, 435 (1968) Novosibirsk, USSR (August 1-7, 1968).

2. D. G. McAlees, N. A. Uckan, E. S. Bettis, C. L. Hedrick, E. F. Jaeger, and D. B. Nelson, "The Elmo Bumpy Torus Reactor (EBTR) Reference Design," Oak Ridge National Laboratory report ORNL/TM-5669 (November, 1976).

3. N. A. Uckan, E. S. Bettis, C. L. Hedrick, R. T. Santoro, H. L. Watts, and H. T. Yeh, "Physics and Engineering Aspects of the EBT Reactor," Proc. 7th Symp. Eng. Problems of Fusion Research, I, 614 (1977).

4. N. A. Uckan, E. S. Bettis, R. A. Dandl, C. L. Hedrick, R. T. Santoro, H. L. Watts, and H. T. Yeh, "The Elmo Bumpy Torus (EBT) Reactor - A Status Report," Proc. 3rd ANS Topical Meeting on the Technology of Controlled Nucl. Fusion I, 74 (1978) Santa Fe, NM (May 9-11, 1978).

5. N. A. Uckan, D. B. Bathelor, E. S. Bettis, R. A. Dandl, C. L. Hedrick, and E. F. Jaeger, "The ELMO Bumpy Torus (EBT) Reactor," Proc. 7th Inter. Conf. on Plasma Physics and Controlled Fusion Research III, 343 (1979), Innsbruck, Austria (August 23-30, 1978).

6. J. T. Woo, N. A. Uckan, and L. M. Lidsky, "Economic Analysis of the EBT Reactor," Proc. 7th Symp. Eng. Problems of Fusion Research, II, 681 (1977).

7. Que-Tsang, Fang, "Self-Consistent Operation of D-T and Advanced Field ELMO Bumpy Torus Reactor," M. S. Thesis, University of Illinois (1979).

8. C. G. Bathke, D. J. Dudziak, R. A. Krakowski, W. B. Ard, D. A. DeFreece, D. E. Driemeyer, R. E. Juhala, R. J. Kashuba, P. B. Stones, L. M. Waganer, D. S. Zuckerman, and D. W. Lieurance, "The Elmo Bumpy Torus Reactor," 4th ANS Topical Meeting on the Technology of Controlled Nuclear Fusion, King of Prussia, PA (October 14-17, 1980).

9. C. G. Bathke, D. J. Dudziak, R. A. Krakowski, W. B. Ard, D. A. Bowers, J. W. Davis, D. A. DeFreece, D. E. Driemeyer, R. E. Juhala, R. J. Kashuba, P. B. Stones, L. M. Waganer, D. S. Zuckerman, D. A. Barry, L. Gize, B. C. Kenessey, J. A. Dela Mora, D. W. Lieurance J. L. Saunders, S. Hamasaki, and H. H. Klein, "Elmo Bumpy Torus Reactor and Power Plant," Los Alamos National Laboratory report LA-8882-MS (August 1981).

10. R. A. Dandl, F. W. Baity, Jr., J. K. Ballou, D. B. Batchelor, E. S. Bettis, D. B. Campbell, and G. L. Campen, "The EBT-II Conceptual Design Study," Oak Ridge National Laboratory report ORNL/TM-5955 (September, 197).

11. D. B. Nelson, and C. L. Hedrick, "Macroscopic Stability and Beta Limit in the ELMO Bumpy Torus," Nucl. Fusion 19, 283 (1979).

12. J. W. Van Dam and Y. C. Lee, "Stability Analysis of a Hot Electron (EBT) Plasma," Bull. Amer. Phys. Soc. 24, 8, 1048 (October, 1979).

13. L. M. Kovrizhnykh, "Transport Phenomena in Toroidal Magnetic Systems," Sov. Phys. - JETP 29, 475 (1969).

14. C. L. Hedrick, E. F. Jaeger, D. A. Spong, G. E. Guest, K. A. Krall, J. B. McBride, and G. W. Stewart, Nucl. Fusion 17, 1237 (1977).

15. E. F. Jaeger, C. L. Hedrick, and D. A. Spong, "Radial Transport in the ELMO Bumpy Torus in Collisionless Regimes," Oak Ridge National Laboratory report ORNL/TM-6806 (April, 1979).

16. E. F. Jaeger, and C. L. Hedrick, "Radial Transport in the ELMO Bumpy Torus in Collisional Regimes," Nucl. Fusion 19, 443 (1979).

17. R. D. Hazeltine, N. A. Krall, H. H. Klein, and P. J. Catto, "Neoclassical Transport in EBT," Science Applications, Inc. report SAI 2379-664LJ (1979).

18. D. A. Spong and C. L. Hedrick, "Variational Corrections to ELMO Bumpy Torus Neoclassical Ion Transport," Phys. Fluids 23, 1903-1914 (1980).

19. L. A. Berry, C. L. Hedrick, and N. A. Uckan, "ELMO Bumpy Torus," Oak Ridge National Laboratory report ORNL/TM-6743 (March, 1979).

20. C. C. Baker (Principal Investigator) et al., "STARFIRE - A Commercial Tokamak Fusion Power Plant Study," Argonne National Laboratory report ANL/FPP-80-1 (September, 1980).